ARCHIVES of FOUNDRY ENGINEERING

Published quarterly as the organ of the Foundry Commission of the Polish Academy of Sciences

ISSN (1897-3310)
Volume 13
Special Issue
2/2013

18 – 21

3/2

Partially Melted Zone in Mg-Al Type Alloy After Gas-tungsten Arc Welding

K.N. Braszczyńska-Malik [a,] *, E. Przełożyńska [a], M. Mróz [b]
[a] Institute of Materials Engineering, Czestochowa University of Technology,
Al. Armii Krajowej 19, 42-200 Czestochowa, Poland
[b] Rzeszow University of Technology, Departament of Casting and Welding,
St. W. Pola 2, 35-959 Rzeszow, Poland
*Corresponding author. E-mail address: kacha@wip.pcz.pl

Received 08.07.2013; accepted in revised form 09.09.2013

Abstract

The gas-tungsten arc (GTA) welding behaviors of the commercial AZ91 magnesium alloy were examined in terms of microstructure characteristics. This study focused on the effects of the GTAW process parameters (like welding current, welding speed and method of additional cooling of the welded samples) on the size of the fusion zone (FZ) and partially melted zone (PMZ). The PMZ morphology of the eutectic regions changed from less to more divorced in the direction from the FZ to the base metal. The largest PMZ was obtained at a low welding speed (3.33 mm/s) and without additional water cooling of the samples.

Keywords: Mg-Al-Zn alloy, Gas-tungsten arc welding, Partially melted zone

1. Introduction

Recently, the welding technology of magnesium alloys, including friction stir welding, tungsten inert gas (TIG) welding, laser hybrid welding or electron-beam welding processes, have been investigated widely [1-8]. One of these methods is also gas-tungsten arc (GTA) welding [9-11], which has been used extensively for the advantages of utility and economy (i.e. short processing time, flexibility of operation, economy in time, energy and material consumption and processing precision). The GTA welding technique also requires only a low cost for equipment investment. Additionally, GTA welding produces very high quality welds as opposed to other methods, thus minimizing the complicating effects arising from weld defects such as porosity, undercuts and weld spatter. Earlier studies [11] allowed one to determine the effects of GTA welding process parameters (like welding current and welding speed) on the energy absorption by the substrate material. The dependences of arc and welding efficiency on the used process parameters were presented. In the present work, the depth and microstructure of the partially melted zone in the AZ91 magnesium alloy employing the GTA welding process was presented.

2. Experimental procedures

Commercial ingots of AZ91 magnesium alloy were used as the starting material. The nominated chemical composition of the AZ91 alloy according to the ASTM B93-94 standard is given in Table 1. Welding plates were machined to the size of 250 x 50 x 15 mm. The gas-tungsten arc (GTA) welding method was conducted by using a Falting 315 AC/DC instrument, described in [11], with and without water flow. A set of 2.4 mm diameter tungsten electrodes were used (WT20 according to the DIN Standard). The shielding gas was helium with a flow rate of 20 l/min.

Table 1.
Chemical composition of AZ91 alloy according to ASTM B93-94

Alloy	Chemical composition [wt.%]*		
	Al	Zn	Mn
AZ91	8.5-9.5	0.45-0.9	0.17-0.4

*Mg rest (Impurities: Si – max 0.05, Fe – max 0.005, Cu – max. 0.003, Ni – max. 0.002, others – max. 0.02)

The specimens for microstructure investigations were prepared by standard metallographic procedures including wet pre-polishing and polishing with different diamond pastes without contact with water. The samples were etched in a 1% solution of HNO_3 in C_2H_5OH for about 60 s. The microstructure was observed using light (Axiovert 25, CarlZeiss-Jena) and scanning electron microscopy (JSM-6610LV, Joel) techniques.

3. Results and discussion

Fig. 1 shows a typical microstructure of the as-cast AZ91 alloy (base material). It indicates that the AZ91 alloy is mainly composed of the dendrite phase – a primary α solid solution of the alloying elements in magnesium (points A and B in Fig. 1) and divorced eutectic in the interdendritical spaces. Strong dendritic segregation of the alloying elements is characteristic for the majority of as-cast magnesium alloys. In Mg-Al type alloys, the divorced eutectic is composed of a γ-$Mg_{17}Al_{12}$ phase (points E in Fig. 1) and a near-eutectic α phase surrounding the γ phase (points C and D in Fig. 1). The aluminum concentration in point C indicates that a eutectic α phase is also present inside visible γ phase islands. The presence of Zn especially in the γ phase was also revealed. In commercial hypoeutectic Mg-Al alloys (with aluminium contents less than about 10 wt.% Al), the eutectic exhibited morphologies that are generally referred to as fully or partially divorced. Generally, in Mg-Al alloys the eutectic tends to become more divorced with an increasing cooling rate but its morphology also depends on the location of the couple zone and undercooling during solidification. In commercial cast ingots, both types of eutectic are observed depending on the local solidification conditions inside the ingot and also on the depth of the etching reagent penetration [11].

The values of the width and depth of the fusion zone obtained using different GTAW parameters are presented in Table 2. As was described in the previous work [11], fusion zone geometry depends obviously on linear energy (i.e. energy per unit length, which is defined as the quantity of energy incident upon the workpiece per unit length and is given by the ratio of input power to welding speed). Therefore, if the welding power increases or the welding speed decreases, the energy per unit length will rise and at the same time the fusion zone will be wider.

The low-melting point nature of the eutectic, only 710 K (and also of the γ phase – about 723 K) coupled with the high thermal conductivity and low heat capacity of the AZ91 alloy, lead to the formation of a wide partially melted zone (PMZ), which was located from the fusion boundary to the base metal. For all the samples GTA welded with different parameters, partially melted zones were observed. Figs. 2 and 3 show the microstructure of the fusion zone, PMZ and base metal for samples GTA welded at a current of 200 A. In the figures, detailed microphotographs of the microstructure changes from the fusion zone to the base metal are presented. (In Fig. 1b the black areas at the bottom of the image are the stronger etched eutectic regions.)

(a)

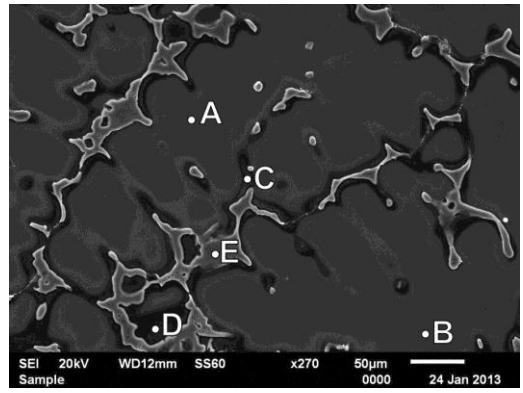

(b)

Point	Chemical composition [wt.%]			Chemical composition [at.%]		
	Mg	Al	Zn	Mg	Al	Zn
A	97.61	2.39		97.84	2.16	
B	96.35	3.65		96.70	3.30	
C	86.97	13.03		88.11	11.89	
D	87.30	11.58	1.11	88.94	10.63	0.42
E	60.57	34.51	4.92	64.78	33.26	1.96

Fig. 1. Microstructure of as-cast AZ91 alloy (base material); SEM (a) and results of EDS analysis for marked points (b)

Table 2.
Applied GTAW parameters with obtained results of geometry of FZ and depth of PMZ

Welding current, I [A]	Welding speed, v_s [mm/s]	Water flow	Width of FZ [mm]	Depth of FZ [mm]	Depth of PMZ [mm]
200	3.33	yes	10.61	2.12	2.24
200	3.33	no	16.22	4.5	7.76
200	13.3	yes	7.47	1.27	1.63
200	13.3	no	10.27	2.37	1.66
300	13.3	yes	10.93	2.49	1.67
300	13.3	no	10.84	3.64	1.73

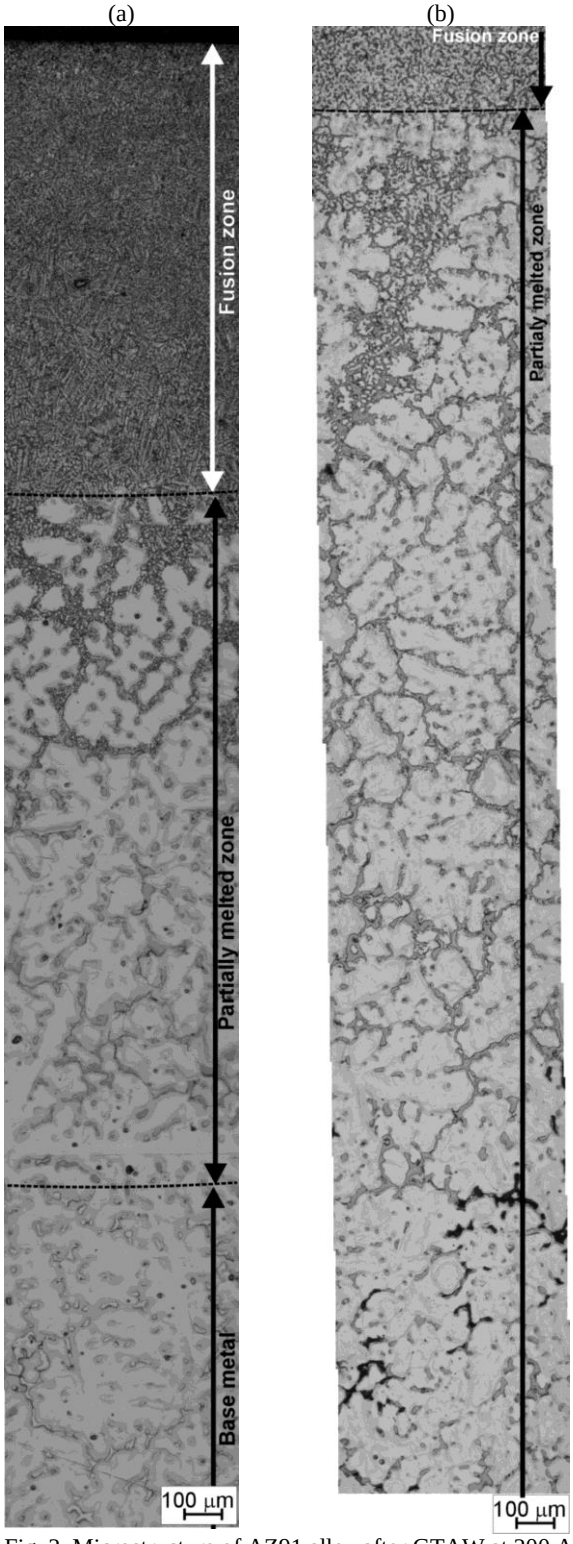

Fig. 2. Microstructure of AZ91 alloy after GTAW at 200 A current and (a) 13.3 mm/s welding speed and (with water flow), (b) 3.33 mm/s welding speed and (without water flow)

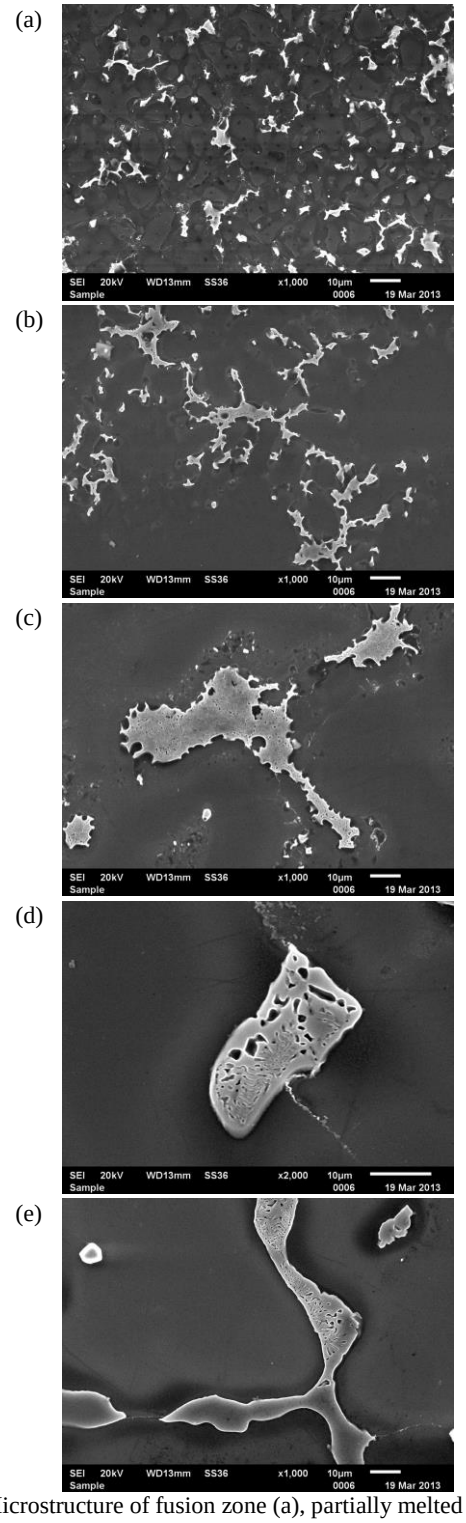

Fig. 3. Microstructure of fusion zone (a), partially melted zone (b-e) and base material (bottom of e image) after GTA welding of AZ91 alloy at 13.3 mm/s welding speed and 200 A current (with water flow), SEM

As can be seen, the PMZ morphology of the eutectic regions changed from less to more divorced in the direction from the fusion zone to the base metal. Additionally, the width of the local remelted areas decreased in this direction. Near the base metal, the amount (and width) of the melted and resolidified eutectic in the PMZ was comparable to the amount of eutectic in the base metal. This indicated that the rate of dissolution in a solid state was low and once melting starts in the PMZ, melting was extensive in the interdendritic regions of the original cast structure. Near the fusion zone, the amount of resolidified areas increased due to the higher temperature during welding. In this region, the remelted areas were visibly wider which indicated that the eutectic α phase surrounding the interdendritical regions was also remelted. Detailed morphology of PMZ is also presented in Fig. 3. The thermal property of the base metal, energy input and cooling rate of the weld determine the temperature distribution established from the fusion boundary to the base metal. The gradient of temperature distribution also determines the depth of the PMZ. As can be seen from a comparison of the values presented in Table 2, the depth of the PMZ corresponded to the dimension of the fusion zone. Although the depth of FZ increase with a rise in welding current, this influence on the depth of PMZ is not so strong. The largest PMZ was obtained at a low welding speed (3.33 mm/s) and without water cooling of the samples. Although the process parameters influence the depth of PMZ, their influence on the morphology in PMZ was not observed. Additionally, significant changes in the chemical composition of the remelted eutectic areas were not revealed (Fig. 4).

(a)

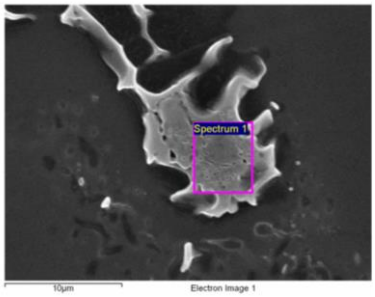

(b)

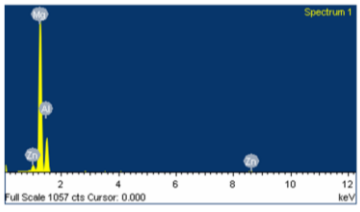

(c)

Element	wt.%	at.%
Mg	63.07	66.80
Al	33.27	31.75
Zn	3.66	1.44

Fig. 4. Microstructure of partially melted zone (a) and SEM+EDX analysis results from observed area (b-c) after GTA welding of AZ91 alloy at 3.33 mm/s welding speed and 200 A current (without water flow)

4. Summary

Due to the low-melting nature of the eutectic in the AZ91 alloy, the presence of a partially melted zone was formed in the alloy after GTA welding. The partially melted zone morphology changes from more to less divorced in the direction from the base metal to the fusion zone. What is more, the width of the local remelted areas decreased in this direction. The welding speed had the largest influence on the depth of the partially melted zone (especially in the samples without additional water cooling from the bottom).

References

[1] Quan, Y. J., Chen, Z. H., Gong, X. J. & Yu, Z. H. (2008). Effects of heat input on microstructure and tensile properties of laser welded magnesium alloy AZ31. *Materials Characterization.* 59, 1491-1497.

[2] Su, S. F., Huang, J. C., Lin, H. K. & Ho, N. J. (2002). Electron Beam Welding Behavior in Mg-Al-Based Alloys. *Metall. Mater. Trans.* 33A, 1461-1473.

[3] Liu, L. & Jiang, J. (2009). The effect of adhesive layer on variable polarity plasma arc weld bonding process of magnesium alloy. *Journal of Materials Processing Tech.* 209, 2864-2870.

[4] Chowdhury, S. M., Chen, D. L., Bhole, S. D., Cao, X., Powidajko, E., Weckman, D. C. & Zhou, Y. (2010). Tensile properties and strain-hardening behavior of double-sided arc welded and friction stir welded AZ31B magnesium alloy, *Mat. Sci. Eng.* 527(A), 2951-2961.

[5] Abderrazak, K., Kriaa, W., Salem, W. B., Mhiri, H., Lepalec, G. & Autic, M. (2009). Numerical and experimental studies of molten pool formation during an interaction of a pulse laser (Nd:YAG) with a magnesium alloy. *Opt. Laser Technol.* 41, 470-480.

[6] Xu, N., Shen, J., Xie, W., Wang, L., Wang, D. & Min D. (2010). Abnormal distribution of microhardness in tungsten inert gas arc butt-welded AZ61 magnesium alloy plates, *Mater. Charact.* 61, 713-719.

[7] Jun, S. & Nan, X. (2012). Effect of preheat on TIG welding of AZ61 magnesium alloy. *International Journal of Minerals, Metallurgy and Materials.* 19, 360-363.

[8] Tashiro, S., Tanaka, M., Nakatani, M., Tani, K. & Furubayashi, M. (2007). Numerical analysis of energy source properties of hollow cathode arc. *Surf. Coat. Technol*. 201, 5431-5434.

[9] Guoli, L. & Shaoqiang, L. Y. (2008). Study on the temperature measurement of AZ31B magnesium alloy in gas tungsten arc welding. *Materials Letters.* 62, 2282-2284.

[10] Munitz, A., Cotler, C., Stern, A. & Kohn, G. (2001). Mechanical properties and microstructure of gas tungsten arc welded magnesium AZ91D plates. *Materials Science and Engineering*. 302, 68-73.

[11] Braszczynska-Malik, K. N. & Mroz, M. (2011). Gas-tungsten arc welding of AZ91 magnesium alloy. *Journal of Alloys and Compounds.* 509, 9951-9958.